

# Calculation of the Steady State Performance for Small Commutator Permanent Magnet DC Motors: Classical and Finite Element Approaches

Mitchell Wing and Jacek F. Gieras, *Senior Member, IEEE*

**Abstract**—Two methods of calculating the steady-state performance of small commutator permanent magnet dc motors are presented here. The finite element and classical methods have been used and compared with experimental data for an 8-W dc motor with segmental permanent magnets. The results have revealed the accuracy and shortcomings of the two methods. The cogging torque calculated using the finite element technique has also been analyzed.

## I. INTRODUCTION

PERMANENT magnet (PM) dc commutator motors have outstanding performance for use in automated manufacturing systems, automobiles, office machine-drives, tools, medical equipment, home appliances etc. Since these machines are manufactured in many different shapes and in large quantities, reliable calculation methods and powerful computer software are required for design purposes.

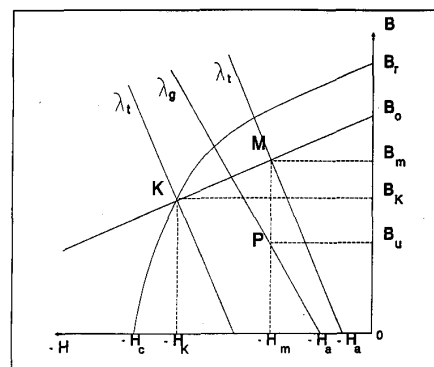
An attempt has been made to study the steady-state performance of a small PM dc motor obtained using two distinct methods: 1) a classical (circuital) approach including analytical approximations of the demagnetization curve and permeance lines to locate the operating point of the permanent magnet, and 2) a finite element technique. PC-based computer software has been used for these two approaches. The cogging torque calculated using the finite element method has also been discussed. The calculated results are compared with those obtained from experimental tests.

## II. CLASSICAL ANALYSIS

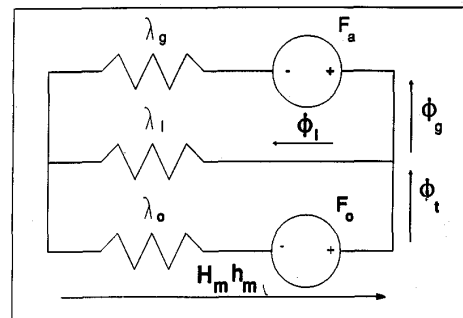
Permanent magnets operate on the demagnetization curve of the hysteresis loop, in the upper left-hand quadrant. (Fig. 1(a)) The demagnetization curve for the majority of hard magnetic materials can be described analytically using, for example, an equation for a hyperbola [1]. To calculate the operating point of a permanent magnet,

Manuscript received August 12, 1991; revised February 27, 1992. This work was supported by the Foundation for Research and Development (FRD) of the Republic of South Africa and by the University of Cape Town. The authors are with the Department of Electrical and Electronic Engineering, University of Cape Town, Rondebosch 7700, Republic of South Africa.

IEEE Log Number 9200164.



(a)



(b)

Fig. 1. Finding the operating point of a permanent magnet system. (a) Demagnetization curve and permeance lines. (b) Equivalent magnetic circuit.

an equivalent magnetic circuit per pole pair is used. (Fig. 1(b)) The various leakages are lumped into an equivalent leakage flux  $\Phi_l$  in a path of permeance  $\lambda_l$ . The useful flux  $\Phi_g$  in the gap permeance  $\lambda_g$  and with an armature reaction (MMF)  $F_a$ , occupies a parallel path. The “open circuit” MMF,  $F_0$ , acting through a permeance  $\lambda_0$ , occupies another parallel path. All the paths with  $\lambda_l$ ,  $\lambda_g$  and  $\lambda_0$  are in parallel.

The magnetic field intensity corresponding to the MMF of the armature reaction is

$$H_a = \frac{F_a}{h_m}, \tag{1}$$

where  $h_m$  is the height of the PM. The useful magnetic

flux density of the magnet is [1]

$$B_u = \frac{\phi_g}{S_m} = -\lambda_g \frac{h_m}{S_m} (H_m - H_a), \quad (2)$$

where  $S_m$  is the cross sectional area of the PM and  $H_m$  is the magnetic field intensity corresponding to the operating point  $M$  (Fig. 1(a)).

The permeances  $\lambda_r = \lambda_l + \lambda_g$  and  $\lambda_g$  are functions of magnetic permeability which depend on the magnetic field intensity. Therefore, the lines of  $\lambda_r$  and  $\lambda_g$  show a slight saturation.

The energy conversion process between the electrical and mechanical quantities is expressed as  $EI = \Omega T$  where  $E$  is the EMF of the motor (rotational EMF),  $I$  is the armature current,  $T$  is the developed (electromagnetic) torque and  $\Omega = 2\pi n$  is the rotor angular speed (rad/s).

The steady-state performance is found with the aid of Fig. 1(a) and the fundamental dc machine equations; i.e., for the armature electric circuit, for the EMF and for the developed torque. The brush voltage drop  $\Delta V_{br}$  is assumed to be constant and thus independent of armature current.

The output power is the difference between the input power and the losses (i.e., armature winding losses, brush-drop losses, rotor rotational losses, armature core losses and stray losses). Stray load losses are assumed to be 1% of the output power. The method of calculating the rotational losses for small electrical motors is described in monograph [2].

### III. FINITE ELEMENT ANALYSIS

The machine is analyzed on the assumption that it has infinite axial length ( $z \rightarrow \infty$ ). A two-dimensional model ( $x$  and  $y$  axis) is thus used with the added assumption that the slot current density is axially directed,  $\vec{J} = \vec{I}_z J(x, y)$ , with a resultant axially directed magnetic vector potential, i.e.,  $\vec{A} = \vec{I}_z A(x, y)$  where  $\vec{I}_x = \mathbf{0}$ ,  $\vec{I}_y = \mathbf{0}$ ,  $\vec{I}_z$  are unit vectors. The nonlinear Poisson's equation subject to the appropriate Dirichlet and homogenous Neumann boundary conditions has been solved numerically [3], [4], [5].

The developed output torque is calculated using the method of virtual work [6], [7], [8], i.e.:

$$T(\theta) = \frac{W_c(\theta + \Delta\theta) - W_c(\theta)}{\Delta\theta} * MF * L_m, \quad (3)$$

where  $W_c$  is the coenergy,  $\theta$  is the rotor angle in radians ( $\Delta\theta$  typically 0.2 degrees),  $MF$  is the model factor,  $L_m$  is the effective length of the rotor stack. The model factor  $MF = 2$  for a half model simulated and  $MF = 4$  for a quarter model. Some authors, e.g., [6], say that this approach is unreliable. On the other hand (3) has been successfully used by many researchers, e.g., [7], [8], [9].

The mechanical output torque is calculated from the developed electromagnetic torque subtracting the torque corresponding to the rotational losses.

The armature core losses have been neglected, due to their insignificance in the general performance character-

istics. The rotor angular speed is calculated from as:

$$\Omega = (V - \Sigma R_a - V_{br}) \left( \frac{I}{T} \right) \quad (4)$$

where  $\Sigma R_a$  is the resistance of the armature circuit.

### IV. RESULTS

The design data of the motor are shown in Table I. The results from classical machine theory and the finite element technique are both compared against experimental results. The finite element mesh for the analyzed 8-W motor is shown in Fig. 2. The magnetic flux distribution using the finite element method is shown in Fig. 3(a) and Fig. 3(b). The torque versus armature current, input power, output power and efficiency are shown in Figs. 4–7. Cogging torque versus rotor angle is plotted in Fig. 8.

The material characteristics, including the demagnetization curve of the PM, are set within the programs. The silicon steel of the rotor and the mild steel of the stator yoke (frame) are both analyzed as being nonlinear.

#### A. Classical Calculation

The graphs shown in Figs. 4–7 show discrepancies between the results of the classical approach and the experiments. The greater errors occurred in the input parameters like input power and armature current with errors of up to 49%.

The deviations in the results can be attributed to a number of possible reasons. The two most prominent reasons for the errors are 1) the classical method of calculation is based on a one-dimensional model. For small electrical machines the edge effects are significant and cannot be neglected. 2) the magnetic flux density versus magnetic field intensity (B–H) curve, for the PM, supplied with the motor is a general B–H curve for this type of magnetic material given in a catalog and may not truly represent the B–H curve of this specific magnet used in the motor. 3) The operating point on the demagnetization B–H curve of the PM is affected by the armature reaction (MMF) which is not accurately taken into account [1].

#### B. The Finite Element Simulation Results

The outer boundary of the stator yoke has been set to  $A = 0$ , using single point constraints (SPC) on all the outer nodes. A periodic boundary condition is set up one pole pitch apart, with a value of  $-1$ . This is called a multipoint constraint (MPC).

The load is applied as a constant current density in the elements that represent the slots. The load represents the forcing function within the functional energy equation of the model.

The developed torque is calculated by rotating the rotor through 18 steps. Every second increment is only stepped half a degree. This means that the torque is calculated for 9 specific rotor positions at five-degree intervals.

The two dimensional model used in this simulation is in some respects an over simplification. This applies par-

TABLE I  
DESIGN DATA OF A SMALL DC PERMANENT MAGNET MOTOR DRIVING AN  
AUTOMOBILE BLOWER

Rated power	$P_{out} = 8 \text{ W}$
Terminal voltage	$V = 24 \text{ V}$
Number of pole pairs	$p = 1$
Number of parallel path pairs	$a = 1$
Outer diameter of rotor	$D_{2out} = 41 \text{ mm}$
Airgap	$g = 0.7 \text{ mm}$
Thickness of stator yoke	$d_y = 1.5 \text{ mm}$
Height of permanent magnet	$h_m = 8 \text{ mm}$
Length of permanent magnet	$L_m = 25 \text{ mm}$
Overlap angle of magnet (Fig. 8)	$\beta = 1.832 \text{ rad}$
Number of armature turns	$N = 1120$
Number of armature slots	$Z_2 = 8$
Number of commutator segments	$K = 8$
Stacking factor	$k_i = 0.96$

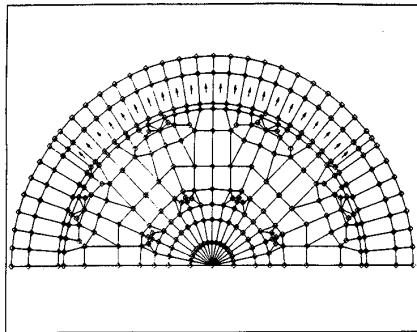
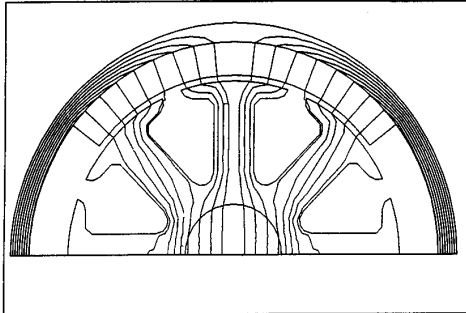
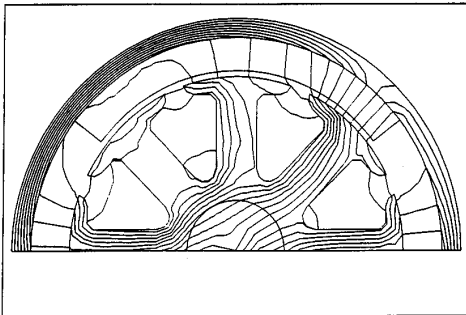


Fig. 2. Finite element mesh of dc permanent magnet motor used by finite element program.



(a)



(b)

Fig. 3. Flux distribution of 8-W dc motor obtained by finite element technique. (a) No load armature current. (b) Stopped rotor armature current.

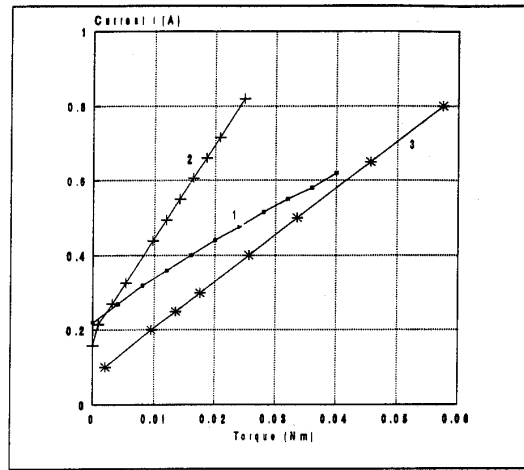


Fig. 4. Armature current versus output torque. 1: text results. 2: Circuital method. 3: Finite element technique.

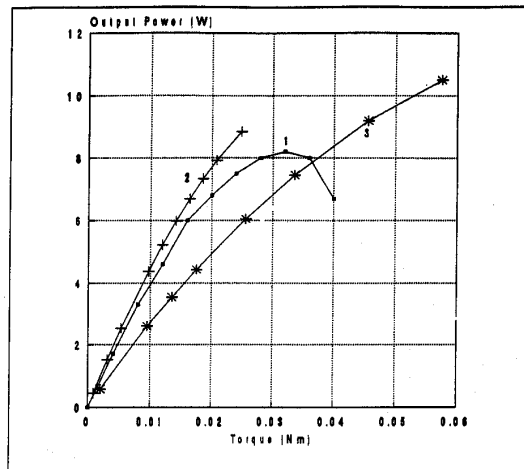


Fig. 5. Output power versus output torque. 1: Text results. 2: Circuital method. 3: Finite element technique.

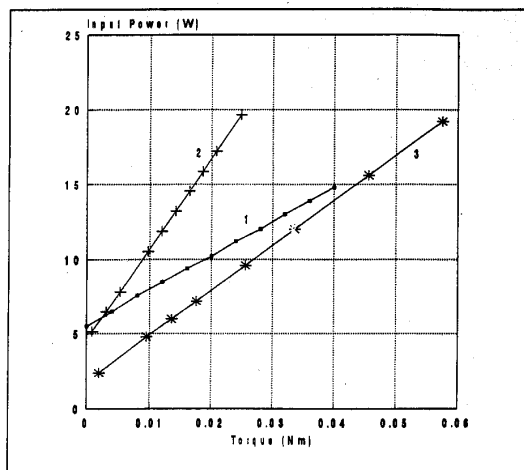


Fig. 6. Input power versus output torque. 1: Text results. 2: Circuital method. 3: Finite element technique.

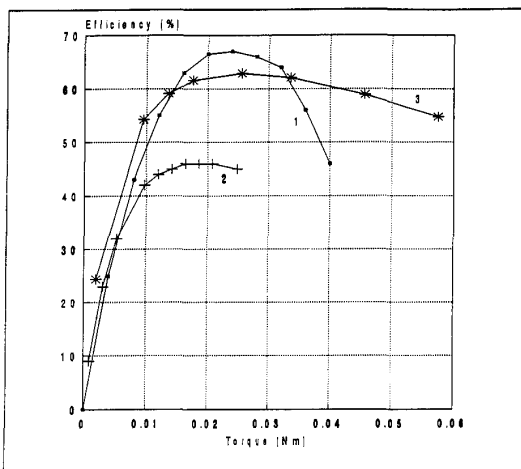


Fig. 7. Efficiency versus output torque. 1: Text results. 2: Circuitual method. 3: Finite element technique.

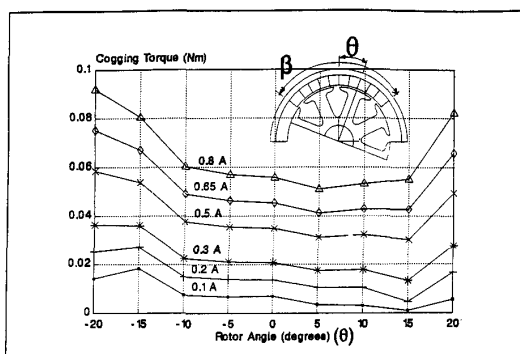


Fig. 8. The cogging torque calculated by the finite element technique over a range of rotor angles  $\theta$ .

ticularly to the stator yoke which has a longer length than the rotor [10] and for this reason has been thickened by 50% to compensate for any unrealistic increases in magnetic flux density.

The finite element results as seen in Figs. 4–7 show an improvement in permanent magnet dc motor calculations. In application to small PM motors the errors from the finite element technique are smaller than those from the classical method only for the output power is the error greater, i.e., up to 32% for the finite element technique, in comparison to 24% for the classical method. However, this conclusion cannot be generalized.

The errors in the simulation can be identified in a number of areas: 1) The finite element model is a two-dimensional model and for this reason the stator yoke of the model had to be thickened to take into account the yoke magnetic flux paths outside the permanent magnet [10]. This could lead to the MMF not being accurately calculated and thus an error in the results. 2) The B–H curve approximation is not accurate. 3) The current density within the slots is assumed to be constant and the slots are simulated as single layer windings although, whereas in

fact, they are double layer windings. 4) Evaluation of losses is not accurate.

### C. Cogging Torque

Small dc motors with slotted rotors show a torque ripple, called cogging. The fewer the slots, the greater the magnetic flux pulsations and cogging torque. The cogging effect is particularly undesirable when a motor runs at low speeds. The considered motor has 8 slots in the rotor. The cogging torque is seen to have the greatest influence at low armature currents, varying up to 90% of the average torque, and having less influence close to rated current of up to 60% of the average torque. Since the number of slots in the rotor is small, the torque ripple is significant.

## V. CONCLUSION

The results show that the finite element technique has a better accuracy over the classical method in calculating the torque using the virtual work principle, armature current, input power, and efficiency of small PM motors. Only the output power–torque characteristics are more accurate using the circuitual approach. The cogging torque can be calculated easily using the finite element technique. The classical method is, however, much quicker and efficient at finding the performance characteristics and the time saved may outweigh the extra time spend using the finite element technique.

## REFERENCES

- [1] J. F. Gieras, "Performance calculation for small DC motors with segmental permanent magnets," *Trans. S. Afr. Inst. Elec. Eng.*, vol. 82, no. 1, pp. 14–21, 1991.
- [2] N. P. Ermolin, *Calculation of Small Commutator Machines*, (in Russian), Moscow: Energia, 1973.
- [3] J. R. Brauer, ed., *What Every Engineer Should Know About Finite Element Analysis*. New York: Marcel Dekker, 1988.
- [4] P. Silvester, "Finite element solution of saturable magnetic field problems," *IEEE Trans. Power App. Syst.*, vol. PAS-89, no. 7, pp. 1642–1651, 1970.
- [5] F. A. Fouad, T. W. Nehl, and N. A. Demerdash, "Permanent magnet modelling for use in vector potential finite element analysis in electrical machinery," *IEEE Trans. Magn.*, vol. MAG-17, no. 6, pp. 3002–3004, 1981.
- [6] J. L. Coulomb and G. Meunier, "Finite element implementation of virtual work principle for magnetic or electric force and torque computation," *IEEE Trans. Magn.*, vol. MAG-20, no. 5, pp. 1894–1896, 1984.
- [7] J. R. Brauer, E. A. Aronson, K. G. McCaughey, and W. N. Sullivan, "Three dimensional finite element calculation of saturable magnetic fluxes and torques of an actuator," *IEEE Trans. Magn.*, vol. 24, no. 1, pp. 455–458, 1988.
- [8] T. Kabashima, A. Kawahara, and T. Goto, "Force calculation using magnetizing currents," *IEEE Trans. Magn.*, vol. 24, no. 1, pp. 451–454, 1988.
- [9] M. Marinescu and N. Marinescu, "Numerical computation of torques in permanent magnet motors by Maxwell stress and energy method," *IEEE Trans. Magn.*, vol. 24, no. 1, pp. 463–466, 1988.
- [10] T. Kenjo and S. Nagamori, *Permanent-Magnet and Brushless dc Motors*. New York: Oxford University Press, 1985.

Mitchell Wing, was born in Yorkshire, England in December 1968. He received the BSc degree in electrical engineering from the University of Cape Town, Rondebosch, South Africa, in 1990.

He is presently a Research Assistant studying towards his M.Sc. in electrical engineering at the University of Cape Town. His research area is finite element analysis and dc PM electrical motors.

**Jacek F. Gieras**, (M'84-SM'91) received the M.Sc. degree in electrical engineering from the Technical University of Lodz, Poland, the Dr.-Eng. and Dr. habil. degrees, also in electrical engineering, from the Technical University of Poznan, Poland, in 1971, 1975, and 1980, respectively.

He joined the Department of Electrical and Electronic Engineering at the University of Cape Town, Rondebosch, South Africa, in September 1989. His research area is electrical machinery, electromagnetic devices, and electromagnetic field theory. The most extensive research pertains to linear induction motors. He is an author or co-author of more than 100 scientific and technical papers published in many countries, including the USA, the United Kingdom, Germany, and Japan. He has taught and done research in Poland, Czechoslovakia, Canada, and Jordan. In 1987 he was promoted, in Poland, to the rank of Professor.

---